Gas Hydrate Thermodynamic Inhibition with MDEA for Reduced MEG Circulation

Masoumeh Akhfash[a], Mosayyeb Arjmandi[a], Zachary M. Aman[a], John A. Boxall[b], Eric F. May[a,*]

a. Fluid Science & Resources Division, School of Mechanical and Chemical Engineering, University of Western Australia, 35 Stirling Highway, Crawley, WA 6009, Australia

b. Chevron Energy Technology Company Pty Ltd.

Abstract

In the production of natural gas, (mono-)ethylene glycol (MEG) is commonly added to the well stream to prevent the formation of clathrate natural gas hydrates. A reduction in the amount of MEG required for hydrate prevention in industrial subsea flowlines would decrease the costs associated with natural gas production. Methyldiethanolamine (MDEA) is sometimes used for corrosion control in wet gas flowlines by increasing the solution pH, and will be typically injected with the MEG. In systems where both hydrate and corrosion control is required, hydrate inhibition via MDEA could represent an opportunity to reduce the required MEG injection rate. However, no experimental data are available to quantify the degree to which MDEA may act as a hydrate inhibitor, either in isolation or in the presence of MEG. In this work, we report 20 measurements of the hydrate phase boundary in the presence of MDEA (3 to 7 vol%) and MEG (0 or 20 vol%), performed at high pressure (6 to 9 MPa) in a sapphire autoclave cell with both ultra-high purity methane and a natural gas mixture. The results illustrate that MDEA acts as a hydrate inhibitor and, when combined

with MEG, provides additional inhibition. For the systems studied, the effectiveness of MDEA as a hydrate inhibitor is approximately half that of MEG. When 20 vol% MEG was added to the aqueous phase, the MDEA became less effective as a hydrate inhibitor. However, 7 vol% MDEA still caused an average temperature shift in the hydrate phase boundary of 0.3 K, which is equivalent to the effect that would be achieved by increasing the amount of MEG in the system by 3 % (i.e. from 20 vol% to 20.6 vol% MEG).

1 Introduction

Gas hydrates are crystalline inclusion compounds, where molecular cages of water surround species with low molecular weight (e.g. methane)[1]. Natural gas hydrates can form a stable, solid aqueous phase at temperatures up to 20 ℃ for systems under moderate pressure (e.g. > 5 MPa, depending on the gas phase composition). Hydrate formation and blockage in long subsea tie-backs, which are used increasingly to develop and produce natural gas from remote offshore reservoirs, is a major flow assurance risk[2]. Traditionally, gas hydrates in production operations are managed through the injection of thermodynamic hydrate inhibitors (THIs), such as (mono)ethylene glycol (MEG), which form hydrogen bonds with water molecules through their OH-groups. This decreases the hydrate stability temperature at a given pressure as fewer water molecules have hydrogen bond sites available to form hydrate structures[1]. For economic and environmental reasons, MEG must be recovered and recycled at the processing facility. As such, reductions in the amount of MEG required for hydrate prevention would decrease the capital and operating costs associated with MEG injection and regeneration[3-5].

The presence of acid gas compounds (H_2S or CO_2) and water in the produced natural gas can cause corrosion issues. A common corrosion control technique used in such situations is known as pH stabilisation, in which chemicals are injected lead to increase in the pH of the liquid aqueous phase present[6-12]. Doing so facilitates the formation of a protective iron carbonate or sulfide film on the pipeline's internal surface, suppressing corrosion of the steel[11]. Aqueous solutions of methyldiethanolamine (MDEA) are commonly used to lower the pH of formation water in natural gas production flowlines [8, 13, 14].

The parallel injection of chemical inhibitors to prevent hydrate formation and corrosion provides an opportunity to reduce the total amount of inhibitor injected if at least one of the chemicals can suppress both hydrate formation and corrosion. The alkanolamines used for

natural gas sweetening have been reported to inhibit hydrate formation in amine units too[15]. Burgazli et al [16] assessed the dual inhibition effects of four chemicals on corrosion rates and gas hydrate formation using a high-pressure autoclave and a linear polarization resistance meter. However, while the use of MDEA[8, 13, 14] along with MEG in gas flowlines for the control of corrosion and hydrate formation is well established in industrial practice [11], to the best of our knowledge, there are currently no experimental data available to test whether MDEA also acts as a thermodynamic hydrate inhibitor. If MDEA when added to the aqueous MEG solution also acts to suppress the hydrate stability curve, there may an opportunity to reduce the required MEG injection rate. In this paper we present hydrate dissociation data measured in the pressure range (6 to 9) MPa for systems of methane + water + MDEA (at 3 and 7 vol%) and a multi-component gas mixture + water +MDEA (7 vol%) + MEG (0 and 20 vol%).

2 EXPERIMENTAL SECTION

The information on the test materials used in this work is listed in Table 1 and Table 2. Ethylene glycol (99.8%) and n-methyldiethanolamine (>99%) were purchased from Sigma-Aldrich. Ultra-high purity methane (99.995%) and a gas mixture (Table 2) were supplied by Coregas. Deionised water with a conductivity of 0.23 μS was prepared in the laboratory using a Millipore Q purification system. In each test, appropriate quantities of n-methyldiethanolamine, ethylene glycol and deionized water were weighed on an electronic analytical balance with an uncertainty of ±10 mg, and mixed to make an aqueous solution with a volume of about 100 mL at the desired concentration.

Table 1. List of the material used in this experiment

Component	Purity	Supplier	CAS Number
ethylene glycol (1,2-ethanediol)	99.8 wt%	Sigma Aldrich	107-21-1
n-methyldiethanolamine (2,2′-methyliminodiethanol)	≥ 99 wt%	Sigma Aldrich	105-59-9
methane	≥99.995%	Coregas	74-82-8
gas mixture	See Table 2	Coregas	-
De-ionized water	Conductivity of 0.23 µS	Millipore Q purification system	-

Table 2. Composition of the gas mixture used in this experiment

Component	Composition	Uncertainty
ethane	5.71 mol%	0.11 mol%
propane	1.90 mol%	0.04 mol%
carbon dioxide	2.00 mol%	0.04 mol%
methane	Balance	-

A high-pressure visual autoclave (HPVA) apparatus (Figure 1) was used for these experiments. The HPVA apparatus has been described in detail previously[17-19] and only a summary is presented here. It consisted of a sapphire cell (25.4 mm internal diameter, 150 mm height and 6.4 mm thickness, 21.0 MPa rating) with a high pressure magnetically-coupled mixing shaft (MRK Mini 100-50) connected to a ViscoPakt Rheo-57 motor. The motor was capable of producing mixing speeds up to 1800 RPM, with a tolerance in practice of ± 1 RPM. The cell's contents were mixed by a four-blade vane-and-baffle geometry impeller to provide adequate mixing while maintaining a stratified gas-liquid interface. Cell and bath temperatures were measured with 100 Ω platinum resistance thermometers (PRT)

with an uncertainty of 0.15 K and 0.2 K, respectively, while cell and reservoir pressures were monitored by two Omegadyne transducer (0-34.5 MPa, 0-17.3 MPa, respectively) with a uncertainty of 0.01 MPa. Signals from the PRTs, pressure transducers, and torque sensor (up to 57 N·cm with 0.04 N·cm resolution) were recorded by a LabView® data acquisition system at 30 second intervals throughout the experiment. The autoclave cell and gas manifold (12.0 MPa rating) were submerged in a water-glycol bath (1:1 by volume), which contained a ThermoFisher immersion cooler that operated continuously to remove heat. The bath was fitted with an 1100 W electrical cartridge heater, which was activated intermittently by a LabView® control algorithm to maintain cell temperature within a tolerance of 0.15 K.

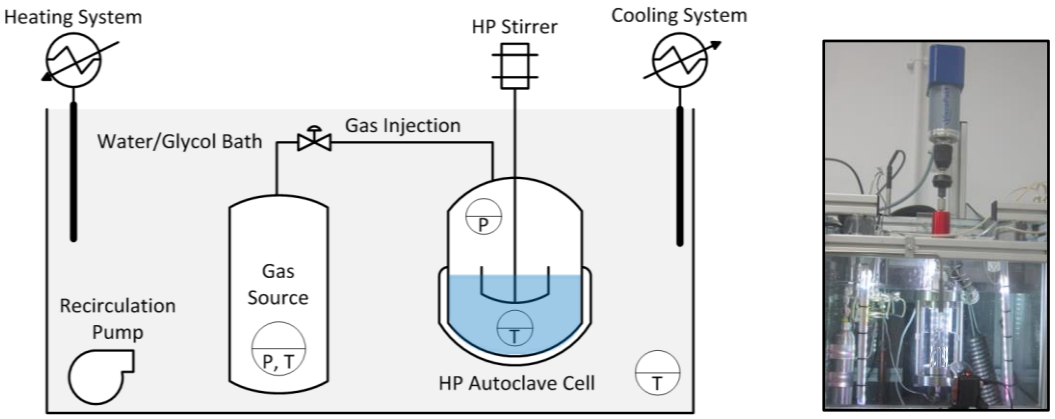

Figure 1. Simplified diagram (left) and picture (right) of the high pressure autoclave cell.

The experimental procedure has been described in detail previously[20]. In each experiment, the cell was thoroughly cleaned with sequential rinses of toluene, ethanol, and acetone, dried overnight, and loaded with water, MDEA and/or the MEG. The cell was then purged with the target gas (methane or gas mixture) three times at 2.0 MPa, and was then pressurised to target starting pressure (6.0, 7.0, 8.0, or 9.0 MPa); the mixing system was engaged at 1000 RPM

with the system outside the hydrate region at 293.15 K. The cell was left overnight to confirm the absence of leaks, and then cooled to 277.15 K at a rate of 1 K/hr. The cell remained inside the hydrate stability region for 20 hours to ensure the hydrate reaction reached steady-state, after which hydrate was dissociated using a step-heating procedure: (i) the cell was heated at 1 K/hr to a point 3 K below the estimated hydrate equilibrium temperature based on Multiflash[21] calculations; (ii) the cell was then heated at 0.1 K/hrs to each temperature step, until the system passed the hydrate equilibrium point. Typically, the system was kept at each step for two to three hours to reach steady-state pressure and temperature; as a consequence, each phase boundary measurement required about three weeks to be completed. The hydrate – liquid – vapour equilibrium condition was determined from each data set by finding the intersection of two straight lines, which were fitted to the gas-liquid data points (most of which were measured during the initial cooling) and the hydrate-gas-liquid data points measured during heating.

A total of twenty experiments were performed in five different systems, as shown in Table 3. The MDEA and MEG volume percent figures shown in Table 3 are based on the water volume only (i.e. in Tests 17-20, 25 ml (27.83 g) of MEG and 7.53 ml (7.82 g) of MDEA were added to 100 ml (100 g) of de-ionised water.

Table 3. The test matrix for experiments to measure the hydrate phase boundaries in the presence and absence of MDEA and MEG.

Test No.	Methane	Gas Mixture	DI Water	MDEA (vol%)	MEG (vol%)	Pressure / MPa
1-4	✓	-	✓	0	0	6.0, 7.0, 8.0, 9.0
5-8	✓	-	✓	3	0	6.0, 7.0, 8.0, 9.0
9-12	✓	-	✓	7	0	6.0, 7.0, 8.0, 9.0
13-16	-	✓	✓	7	0	6.0, 7.0, 8.0, 9.0
17-20	-	✓	✓	7	20	6.0, 7.0, 8.0, 9.0

The standard uncertainties in temperature and pressure of each measured condition were 0.15 K and 0.01 MPa, respectively, while those associated with the determination of the intersection of the two regressed lines were estimated to be 0.21 K and 0.013 MPa, respectively. Combining these in quadrature, we estimate the combined standard uncertainties in the measured equilibrium temperatures and pressures were 0.26 K and 0.02 MPa, respectively.

Figure 2 shows an example of the method used for determining the hydrate dissociation point in the methane–water system. The intersection of the fitted lines to the gas-liquid cooling data points and hydrate-gas-liquid heating data points are found to be 284.91 K and 8.66 MPa. The predicted equilibrium temperature for methane hydrate at 8.66 MPa using the cubic plus association (CPA) equation of state model set in the software package Multiflash[21] is 284.85 K. The deviation of the measured equilibrium temperature at 8.66 MPa from the calculated value using Multiflash[21] is +0.06 K, which is well within the estimated experimental standard uncertainty.

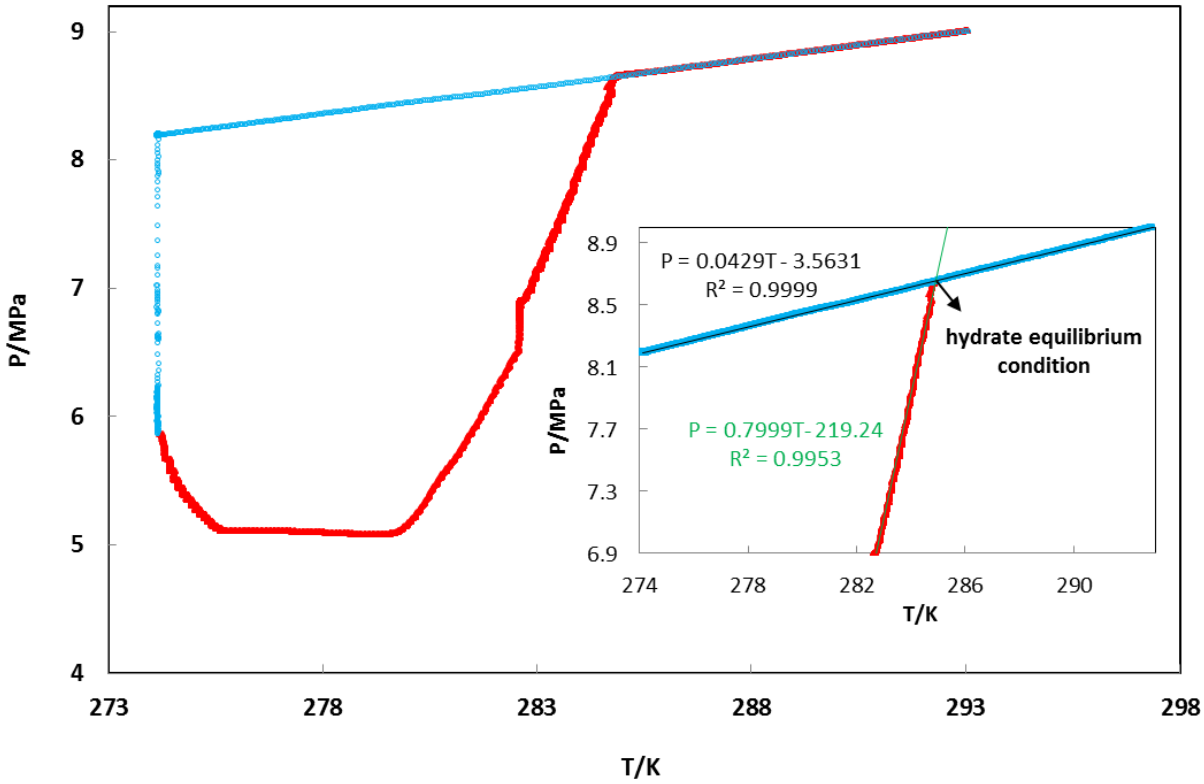

Figure 2. An example of the method used for determining hydrate dissociation points. The intersection of the straight lines fitted to the gas-liquid (methane-water) data points and hydrate-gas-liquid heating data points the hydrate equilibrium condition. The coloured points indicate whether the cell was being cooled (blue) or heated (red).

3 RESULTS AND DISCUSSION

3.1 Methane Experiments

To validate the experimental method and assess the data quality, four tests were carried out with pure methane and deionized water at different pressures. The measured hydrate equilibrium points were then compared to the values measured by others[22-30] and hydrate phase boundary calculated using Multiflash[21] using the cubic plus association (CPA) equation of state model set. The summary of the results is shown in Figure 3 and Table 4, which indicates that our measurements are in very good agreement with the data reported in

literature[22-30] and Multiflash's prediction. The maximum absolute deviation between the measured and calculated temperatures by Multiflash is 0.06 K.

Table 4. Hydrate phase boundary measurements and calculations for methane and water.

P^{exp} / MPa	T^{exp} / K	T^{eq} / K (Calculated)
8.66	284.91	284.85
7.69	283.71	283.75
6.69	282.40	282.43
5.71	280.94	280.90

Standard uncertainties u in temperature T and pressure p are u(T)= 0.26 K and u(p)= 0.02 MPa.

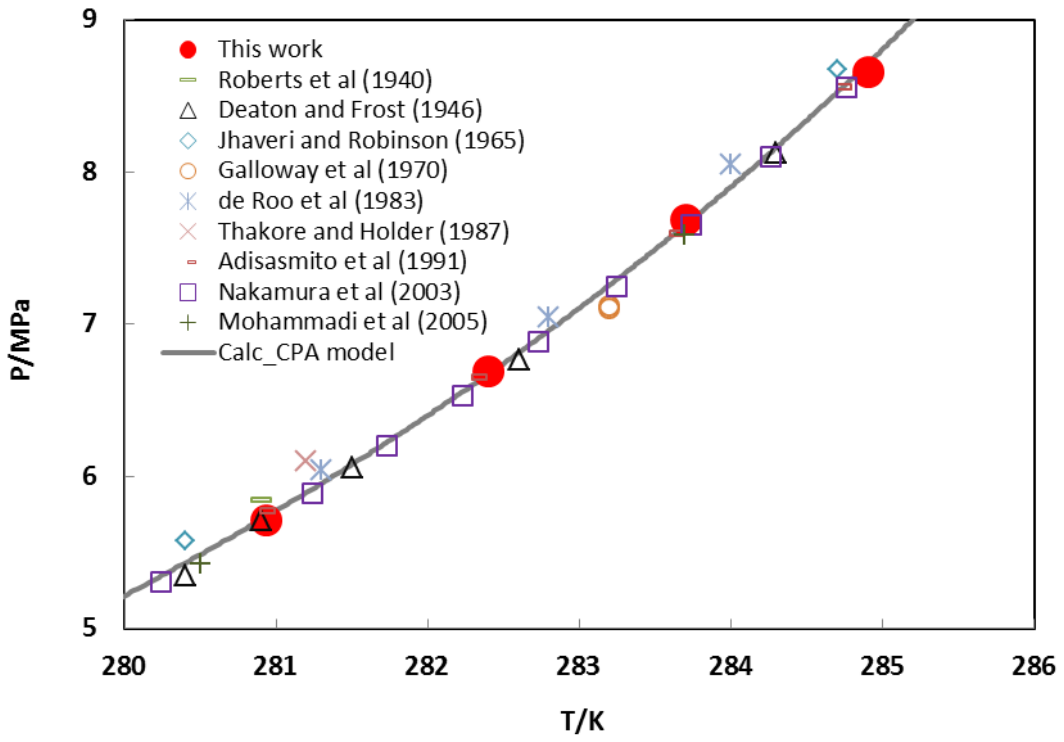

Figure 3. Hydrate phase boundary for methane and water measured in the autoclave (solid red data points), compared to predictions from Multiflash (grey solid curve) and the values measured by others[22-30]. The maximum absolute deviation between the measured and calculated temperatures is 0.06 K.

The effect of adding 3 vol% MDEA to the de-ionised water on the hydrate phase boundary of the methane-water system was measured in the autoclave at pressures ranging from 5.70 to 8.67 MPa. A summary of the results is shown in Figure 4 and Table 5. The addition of 3 vol% MDEA to the aqueous phase inhibited the hydrate phase boundary by an average of 0.3 K; Figure 4 also shows the predicted hydrate phase boundaries for systems with and without 3 vol% MDEA, illustrating that the software package is currently unable to capture the effect of MDEA as a hydrate inhibitor. To quantify this inhibition effect with MDEA, MEG was substituted in the software package to determine the equivalent amount to have the same inhibition effect. The amount of MEG required to shift the methane hydrate phase boundary by approximately 0.3 K was estimated to be 1.5 vol%, as shown in Figure 4; this comparison suggests that, for the pure methane-water system studied, MDEA is approximately half as effective as MEG at hydrate inhibition.

Table 5. Hydrate phase boundary measurements for methane and deionised water containing (3.0 ± 0.1) vol% MDEA.

P^{exp} / MPa	T^{exp} / K	T^{eq} / K (Calculated)	ΔT / K
8.67	284.50	284.85	0.35
7.66	283.36	283.70	0.34
6.69	282.11	282.42	0.31
5.70	280.56	280.87	0.31

Standard uncertainties u in temperature T and pressure p are u(T)= 0.26 K and u(p)= 0.02 MPa.

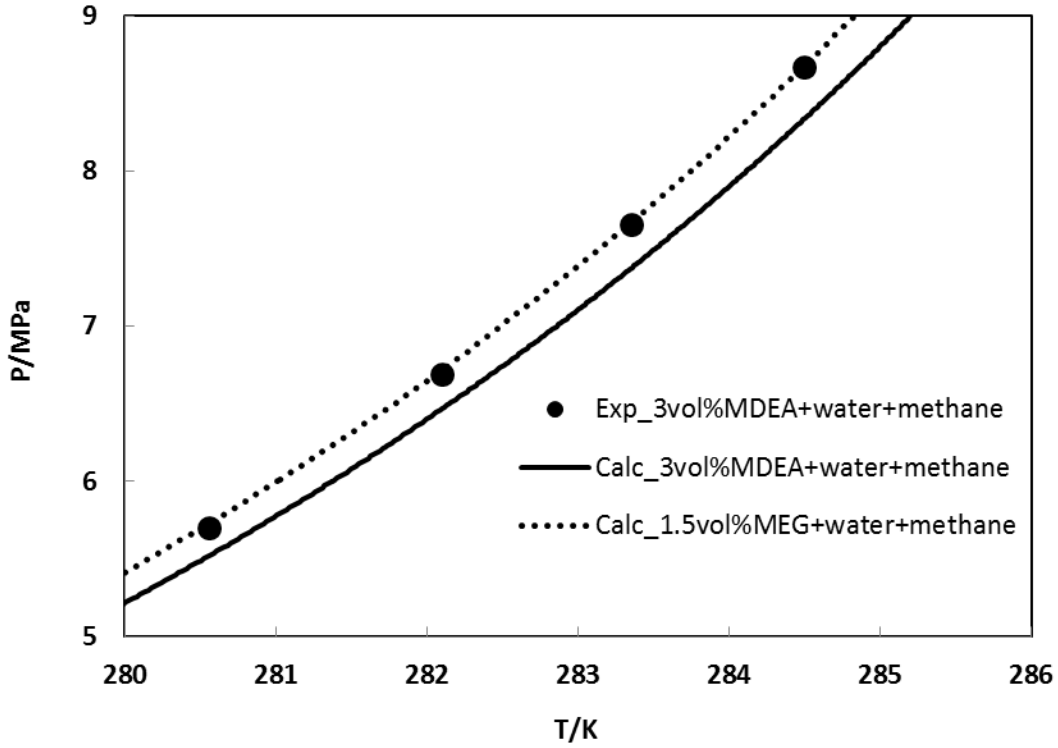

Figure 4. Hydrate phase boundary for methane and an aqueous phase containing 3 vol% MDEA in water, which is represented by circles and corresponds to the experimental measurements in the autoclave, while the solid line correspond to the Multiflash-CPA predictions. The comparison (solid curve and circles) illustrates that the Multiflash model does not account for the effect of MDEA on the hydrate phase boundary. The hydrate phase boundary for methane and an aqueous phase containing 1.5 vol% MEG in water (dotted line) calculated with the Multiflash-CPA model matches (within 0.06 K) the measured hydrate phase boundary for methane and an aqueous phase containing 3 vol% MDEA in water, suggesting 3 vol% MDEA is equivalent to 1.5 vol% MEG.

The effect of 7 vol% MDEA in water on the hydrate phase boundary of the methane-water system was measured in the autoclave at pressures ranging from 5.69 to 8.60 MPa, and a summary of the results is shown in Figure 5 and Table 6. The measured dissociation points show that 7 vol% MDEA shifted the methane hydrate phase boundary by approximately

0.8 K. At these pressure and temperature conditions, the Multiflash[21] calculations suggest that 7 vol% MDEA is equivalent to approximately 3.1 vol% MEG (Figure 5).

Table 6. Hydrate phase boundary measurements for methane and deionised water containing (7.0 ± 0.1) vol% MDEA.

P^{exp} / MPa	T^{exp} / K	T^{eq} / K (Calculated)	ΔT / K
8.60	283.90	284.79	0.89
7.63	282.95	283.68	0.73
6.65	281.57	282.37	0.80
5.69	280.09	280.85	0.76

Standard uncertainties u in temperature T and pressure p are u(T)= 0.26 K and u(p)= 0.02 MPa.

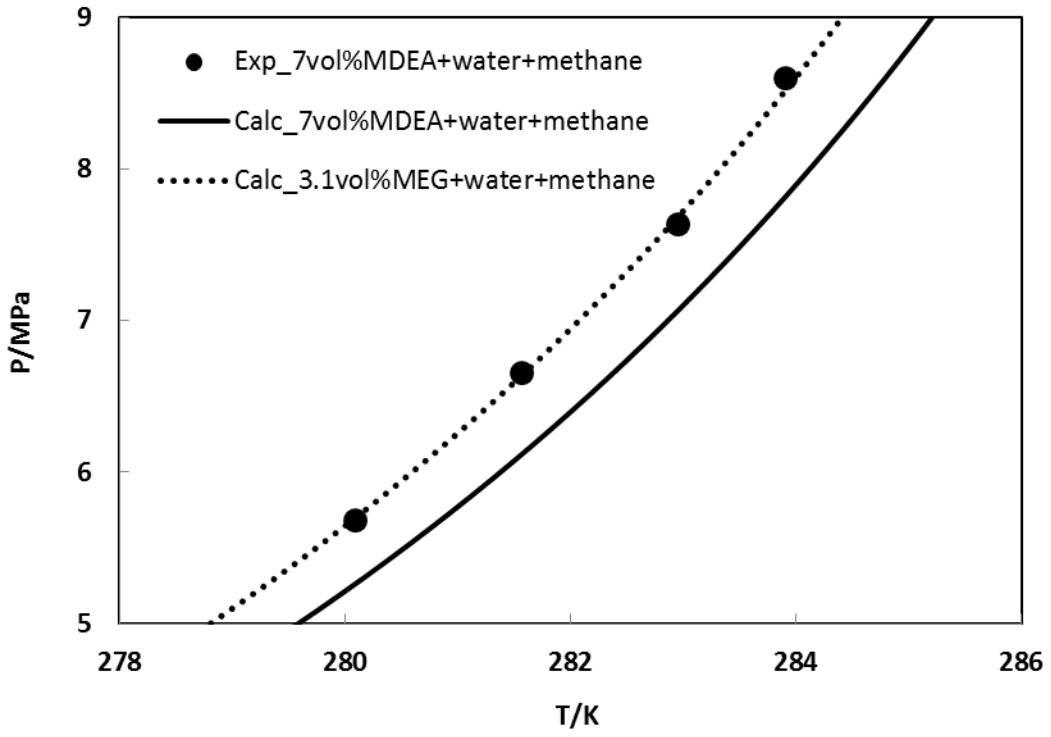

Figure 5. Hydrate phase boundaries for methane and an aqueous phase containing 7 vol% MDEA in water; circles correspond to experimental measurements from the autoclave, while the solid curve corresponds to the Multiflash-CPA predictions, which are almost identical to the predicted phase boundary for methane + water. The calculated hydrate phase boundary for methane and an aqueous phase containing 3.1 vol% MEG (dotted curve) matches (within 0.11 K) the measured hydrate phase boundary for methane and an aqueous phase containing 7 vol% MDEA in water (circles).

3.2 Gas Mixture Experiments

The effect of 7 vol% MDEA in water on the hydrate phase boundary of the mixed gas (Table 2) + water system was measured in the autoclave at pressures ranging from 5.86 to 8.87 MPa, and a summary of the results is shown in Figure 6 and Table 7. The measured dissociation points show that 7 vol% MDEA shifted the hydrate phase boundary for the mixed gas by approximately 0.7 K. At these pressure and temperature conditions, Multiflash[21] calculations suggest that 7 vol% MDEA is equivalent to approximately 3.5 vol% MEG (Figure 6).

Table 7. Hydrate phase boundary measurements for the gas mixture and deionised water containing (7.0 ± 0.1) vol% MDEA.

P^{exp} / MPa	T^{exp} / K	T^{eq} / K (Calculated)	ΔT / K
8.87	290.42	291.13	0.71
7.84	289.51	290.32	0.81
6.81	288.56	289.36	0.80
5.86	287.69	288.28	0.59

Standard uncertainties u in temperature T and pressure p are u(T)= 0.26 K and u(p)= 0.02 MPa.

The effect of an aqueous phase containing 7 vol% MDEA and 20 vol% MEG on the hydrate phase boundary of the gas mixture system was measured in the autoclave at pressures ranging from 5.70 to 8.59 MPa, and a summary of the results is shown in Figure 6 and Table 8. The measured dissociation points indicate that 7 vol% MDEA shifted the mixed gas hydrate phase boundary by approximately 0.3 K. At these pressure and temperature conditions, Multiflash[21] calculations suggest that adding 7 vol% MDEA (relative to the water volume) to a system containing 20 vol% MEG (relative to the water volume) is equivalent to approximately 20.6 vol% MEG (Figure 6). That is the marginal change in the hydrate equilibrium boundary caused by the addition of the MDEA was equivalent to that which would be achieved by a 3 % increase in the amount of MEG above the original concentration.

Table 8. Hydrate phase boundary measurements for the gas mixture and deionised water containing (20.0 ± 0.1) vol% MEG and (7±0.1) vol% MDEA.

P^{exp} / MPa	T^{exp} / K	T^{eq} / K (Calculated)	ΔT / K
8.59	284.40	284.67	0.27
7.61	283.52	283.91	0.39
6.68	282.86	283.05	0.19
5.70	281.66	281.95	0.29

Standard uncertainties u in temperature T and pressure p are u(T)= 0.26 K and u(p)= 0.02 MPa.

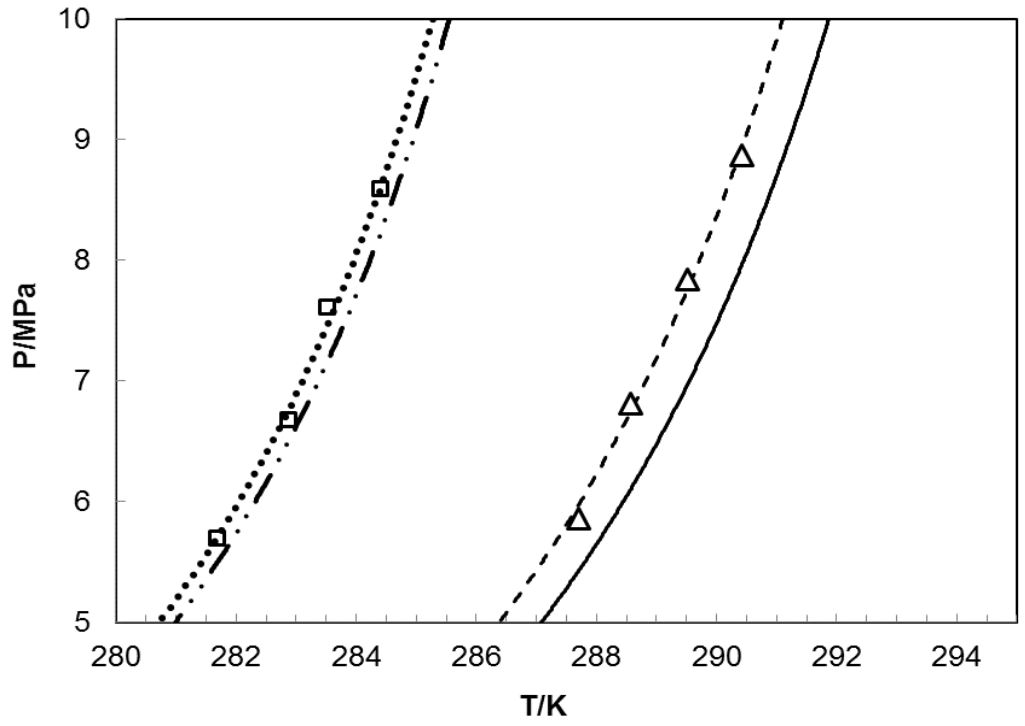

Figure 6. Hydrate phase boundary for the gas mixture and aqueous phases containing various MDEA and/or MEG concentrations in water. Triangle data points correspond to experimental measurements for the system containing 7 vol% MDEA, while the solid curve shows the corresponding Multiflash-CPA predictions, which are insensitive to the presence of MDEA. The calculated hydrate phase boundary for the gas mixture with an aqueous phase containing only 3.5 vol% MEG (dashed curve) matches (within 0.12 K) the measured hydrate equilibrium data for the gas mixture and an aqueous phase containing 7 vol% MDEA in water. The square data points correspond to experimental measurements for the system containing 20 vol% MEG and 7 vol% MDEA in water, while the dashed curve with dots shows the corresponding Multiflash-CPA predictions. The calculated hydrate phase boundary for the gas mixture with an aqueous phase containing only 20.6 vol% MEG (dotted curve) matches (within 0.11 K) the measured hydrate phase boundary for the gas mixture and an aqueous phase containing 20 vol% MEG and 7 vol% MDEA in water (square data points).

4 CONCLUSIONS

The experimental data collected in this investigation demonstrate that MDEA functions as a thermodynamic hydrate inhibitor at the concentrations of (3 and 7 vol%) studied.

Table 9 presents a summary of the results for the methane and mixed gas hydrate phase boundaries measured in the presence of MDEA with and without MEG. The results illustrate that MDEA shifts the hydrate phase boundaries between 0.3 and 0.8 K at these concentrations. This hydrate inhibition effect is not captured currently by industry-standard models for hydrate equilibrium calculation, reflecting the fact that no data for this system were available previously. A comparison between the MDEA experiments and predictions made with the software package Multiflash [21] for MEG-inhibited systems suggested that MEG is approximately twice as effective as MDEA in shifting the hydrate phase boundary to lower temperatures.

Table 9. Summary of the experiments and calculations.

System	Added MDEA (vol%)	Average shift in hydrate curve, ΔT / K	Equivalent MEG (vol%), which causes the same shift in hydrate curve
Methane -Water	0	0	0
	3	0.3	1.5
	7	0.8	3.0
Gas Mixture-Water	7	0.7	3.5
Gas Mixture-Water-MEG (20 vol%)	7	0.3	0.6

In the presence of MEG, MDEA acts to further reduce the hydrate equilibrium temperature. The effectiveness of MDEA as a hydrate inhibitor decreased when it was injected alongside

MEG. For the mixed gas system containing 20 vol% MEG, the addition of 7 vol% MDEA achieved a level of hydrate suppression equivalent to that of 20.6 vol% MEG in water. Thus, the presence of 7 vol % MDEA in a system with 20 % MEG is the equivalent of increasing the amount of MEG injected by 3 % (i.e. the concentration increased in relative terms by 3 %, from 20.0 vol% to 20.6 vol% MEG).

AUTHOR INFORMATION

Corresponding Author

*E-mail: eric.may@uwa.edu.au. Tel.: +61 8 6488 2954. Fax: +61 8 6488 1024

Funding

This work was funded by Chevron Energy Technology Pty Ltd and the Australian Research Council through IC15001019.

Notes

The authors declare no competing financial interest.

ACKNOWLEDEGMENT

The authors would like thank Chevron Energy Technology Pty Ltd. for permission to publish this work, and Prof. Ken Marsh for the donation of the sapphire cell used in this work.

REFERENCES

1. Sloan, E. D.; Koh, C. A., Clathrate Hydrates of Natural Gases. 3rd ed.; CRC Press, Taylor and Francis Group: Boca Raton, FL, 2007.

2. Sinquin, A.; Cassar, C.; Teixeira, A.; Leininger, J. P.; Glenat, P. Hydrate Formation in Gas Dominant Systems, Offshore Technology Conference, Texas, USA, 4-7 May, 2015.

3. Grzelak, E. M.; Stenhaug, M. A More Efficient Use of MEG to Fully Inhibit Hydrates with Reduced Cost, Offshore Technology Conference Asia, Kuala Lumpur, Malaysia, 22-25 March, 2016.

4. Vahedi, S.; Wood, T. Practicalities of Thermodynamic Hydrate Inhibitor Distribution Within 179 Hydrocarbon Systems Under Steady State and Dynamic Operations, 16th International Conference on Multiphase Production Technology, Cannes, France, 12-14 June, 2013.

5. Yang, J.; Vajari, S. M.; Chapoy, A.; Tohidi, B. Minimizing Hydrate Inhibitor Injection Rates, International Petroleum Technology Conference, Kuala Lumpur, Malaysia, 10-12 December, 2014.

6. Dugstad, A.; Seiersten, M.; Nyborg, R. Flow Assurance of pH Stabilized Wet Gas Pipelines, CORROSION 2003, Paper No. 03314, San Diego, USA, 16-20 March, NACE International, 2003.

7. Olsen, S.; Halvorsen, A. M. K. Corrosion Control by pH Stabilization, CORROSION 2015, Paper No. 05733, Dallas, Texas, 15-19 March, NACE International, 2015.

8. Davoudi, M.; Heidari, Y.; Safadoost, A.; Samieirad, S. Chemical Injection Policy for Internal Corrosion Prevention of South Pars Sea-Pipeline: A Case Study. *J. Nat. Gas Sci. Eng.* **2014,** 21, 592-599.

9. deWaard, C.; Lotz, U.; Milliams, D. E. Predictive Model for CO_2 Corrosion Engineering in Wet Natural Gas Pipelines. *Corrosion* **1991,** 47, 976-985.

10. Crolet, J.-L.; Samaran, J. P. The Use of Anti-Hydrate Treatment for the Prevention of CO_2 Corrosion in Long Crude Gas Pipelines, CORROSION 93, Paper No. 102, New Orleans, USA, NACE International, 1993.

11. Nyborg, R. Pipline Corrosion Prevention by pH Stabilization or Corrosion Inhibitors, Rio Pipeline Conference and Exposition 2009, Paper No. IBP1527_09, Rio de Janeiro, Brazil 22-24 September, Brazilian Petroleum, Gas and Biofuels Institute-IBP, 2009.

12. Olsen, S.; Lunde, O.; Dugstad, A. pH-Stabilization in the Troll Gas-Condensate Pipelines, CORROSION 99, Paper No. 19, San Antonio, USA, 25-30 April, NACE International, 1999.

13. Kvarekval, J.; Dugstad, A. Pitting Corrosion in CO_2/H_2S-Containing Glycol solutions Under Flowing Conditions CORROSION 2005, Paper No. 05631, Houston, USA, 3-7 April, NACE International, 2005.

14. Duan, D.; Choi, Y.-S.; Jiang, S.; Nešić, S. Corrosion Mechanism of Carbon Steel in MDEA-Based CO_2 Capture Plants, CORROSION 2013, Paper No. 02345, Orlando, USA, 17-21 March, NACE International, 2013.

15. Carroll, J., Natural Gas Hydrates: A Guide for Engineers. 2nd ed.; Elsevier Science: Gulf Professional Publishing, 2009.

16. Burgazli, C. R.; Navarrete, R. C.; Meas, S. L. New Dual Purpose Chemistry for Gas Hydrate and Corrosion Inhibition *J. Can. Pet. Technol.* **2005,** 44, 47-50.

17. Akhfash, M.; Boxall, J. A.; Aman, Z. M.; Johns, M. L.; May, E. F. Hydrate Formation and Particle Distributions in Gas–Water Systems. *Chem. Eng. Sci.* **2013,** 104, 177-188.

18. Aman, Z. M.; Akhfash, M.; Johns, M. L.; May, E. F. Methane Hydrate Bed Formation in a Visual Autoclave: Cold Restart and Reynolds Number Dependence. *J. Chem. Eng. Data* **2015,** 60, 409−417.

19. Akhfash, M.; Aman, Z. M.; Ahn, S. Y.; Johns, M. L.; May, E. F. Gas Hydrate Plug Formation in Partially-Dispersed Water–Oil Systems. *Chem. Eng. Sci.* **2016,** 140, 337-347.

20. Ward, Z. T.; Johns, M. L.; May, E. F.; Koh, C. A.; Aman, Z. M. Crystal Growth Phenomena of CH_4 + C_3H_8 + CO_2 Ternary Gas Hydrate Systems. *J. Nat. Gas Sci. Eng.* **2016,** 35, 1426-1434.

21. Infochem, Multiflash for Windows 4.2. Infochem Computer Services Ltd.: London, 2012.

22. Roberts, O. L.; Brownscombe, E. R.; Howe, L. Constitution Diagrams and Composition of Methane and Ethane Hydrates. *Oil Gas J.* **1940,** 39, 37-43.

23. Deaton, W. M.; Frost, E. M., Gas Hydrates and Their Relation to the Operation of Natural-Gas Pipe Lines. American Gas Association: United States Bureau of Mines, 1946.

24. Jhaveri, J.; Robinson, D. B. Hydrates in the Methane-Nitrogen System. *Can. J. Chem. Eng.* **1965,** 43, 75-78.

25. Galloway, T. J.; Ruska, W.; Chappelear, P. S.; Kobayashi, R. Experimental Measurement of Hydrate Number for Methane and Ethane and Comparison with Theoretical Values. *Ind. Eng. Chem. Fundam.* **1970,** 9, 237-243.

26. Roo, J. L. D.; C.J. Peters; Lichtenthaler, R. N.; Diepen, G. A. M. Occurrence of Methane Hydrate in Saturated and Unsaturated Solutions of Sodium Chloride and Water in Dependence of Temperature and Pressure. *AIChE J.* **1983,** 29, 651–657.

27. Thakore, J. L.; Holder, G. D. Solid-Vapor Azeotropes in Hydrate-Forming Systems. *Ind. Eng. Chem. Res.* **1987,** 26, 462-469.

28. Adisasmito, S.; Frank, R. J.; Sloan, E. D. Hydrates of Carbon Dioxide and Methane Mixtures. *J. Chem. Eng. Data* **1991,** 36, 68-71.

29. Toshiyuki Nakamura; Makino, T.; Sugahara, T.; Ohgaki, K. Stability Boundaries of Gas Hydrates Helped by Methane Structure-H Hydrates of Methylcyclohexane and Cis-1,2-Dimethylcyclohexane. *Chem. Eng. Sci.* **2003,** 58, 269-273.

30. Mohammadi, A. H.; Anderson, R.; Tohidi, B. Carbon Monoxide Clathrate Hydrates: Equilibrium Data and Thermodynamic Modeling. *AIChE J.* **2005,** 51, 2825-2833.

For Table of Contents Only